The Journal of Experimental Biology 202, 2771–2785 (1999)
Printed in Great Britain © The Company of Biologists Limited 1999
JEB1855



# LOCOMOTION ON THE WATER SURFACE: HYDRODYNAMIC CONSTRAINTS ON ROWING VELOCITY REQUIRE A GAIT CHANGE

ROBERT B. SUTER[1,*] AND HORATIO WILDMAN[2]

[1]*Department of Biology, Vassar College, Poughkeepsie, NY 12604, USA* and [2]*Department of Zoology, Duke University, Durham, NC 27708, USA*

*e-mail: suter@vassar.edu

*Accepted 28 July; published on WWW 30 September 1999*

## Summary

**Fishing spiders, *Dolomedes triton* (Araneae, Pisauridae), propel themselves across the water surface using two gaits: they row with four legs at sustained velocities below 0.2 m s$^{-1}$ and they gallop with six legs at sustained velocities above 0.3 m s$^{-1}$. Because, during rowing, most of the horizontal thrust is provided by the drag of the leg and its associated dimple as both move across the water surface, the integrity of the dimple is crucial. We used a balance, incorporating a biaxial clinometer as the transducer, to measure the horizontal thrust forces on a leg segment subjected to water moving past it in non-turbulent flow. Changes in the horizontal forces reflected changes in the status of the dimple and showed that a stable dimple could exist only under conditions that combined low flow velocity, shallow leg-segment depth and a long perimeter of the interface between the leg segment and the water. Once the dimple disintegrated, leaving the leg segment submerged, less drag was generated. Therefore, the disintegration of the dimple imposes a limit on the efficacy of rowing with four legs. The limited degrees of freedom in the leg joints (the patellar joints move freely in the vertical plane but allow only limited flexion in other planes) impose a further constraint on rowing by restricting the maximum leg-tip velocity (to approximately 33 % of that attained by the same legs during galloping). This confines leg-tip velocities to a range at which maintenance of the dimple is particularly important.**

**The weight of the spider also imposes constraints on the efficacy of rowing: because the drag encountered by the leg-cum-dimple is proportional to the depth of the dimple and because dimple depth is proportional to the supported weight, only spiders with a mass exceeding 0.48 g can have access to the full range of hydrodynamically possible dimple depths during rowing. Finally, the maximum velocity attainable during rowing is constrained by the substantial drag experienced by the spider during the glide interval between power strokes, drag that is negligible for a galloping spider because, for most of each inter-stroke interval, the spider is airborne.**

**We conclude that both hydrodynamic and anatomical constraints confine rowing spiders to sustained velocities lower than 0.3 m s$^{-1}$, and that galloping allows spiders to move considerably faster because galloping is free of these constraints.**

Key words: locomotion, aquatic propulsion, gait, spider, *Dolomedes triton.*

## Introduction

Animals, such as fishing spiders, water striders and basilisk lizards, which run on the surface of water, occupy a locomotor niche that has only begun to be explored empirically (Anderson, 1976; Deshefy, 1981; Glasheen and McMahon, 1996a,b; Gorb and Barth, 1994; McAlister, 1959; Shultz, 1987; Suter et al., 1997). One of the large gaps in our understanding of that locomotor niche concerns the necessity for, and the efficacy of, different gaits.

A gait is a locomotor style that has a circumscribed range of velocities over which it occurs and that is separated from other gaits by discontinuities in the quantities used to describe locomotion (Alexander, 1989). Gait transitions in terrestrial locomotion have received enough attention to allow some understanding of the importance of size (Heglund and Taylor, 1974, 1988) and of the roles played by energetic efficiency and by the tolerance of skeletal materials for stresses. The transition from a slower to a faster gait may result in decreased energetic cost relative to velocity (Alexander, 1989; Hoyt and Taylor, 1981), in increased utilization of the series elastic component of striated muscle (Taylor, 1985), in decreased threat to the integrity of the musculoskeletal system (Biewener and Taylor, 1986; Farley and Taylor, 1991) or in decreased stiffness (=increased compliance) of the legs (McMahon, 1985).

During aquatic locomotion, gait transitions, such as those between pectoral fin and undulatory propulsion (Webb, 1973), have rarely been studied explicitly, although distinct (*sensu* Alexander, 1989) gaits are well recognized (Webb, 1993).

The organisms that live on the water surface, supported there by surface tension, are also known to have distinct gaits: fishing spiders (Arachnida, Araneae, Pisauridae) use rowing and galloping gaits during active locomotion on the water surface and two others during passive locomotion (two forms of sailing: Deshefy, 1981; Suter, 1999); in contrast, whirligig beetles (Insecta, Coleoptera), water striders (Insecta, Hemiptera) and springtails (Insecta, Collembola) are not known to use gaits other than rowing (beetles and water striders) and hopping (springtails) (Anderson, 1976). We have been unable to discover any reports of attempts to elucidate the limitations or energetic costs of gaits in this surface-dwelling guild of arthropods, and we are therefore unaware of any studies of the physiological or biomechanical reasons for the existence of different gaits.

Fishing spiders, *Dolomedes triton* (Pisauridae), the subject of this paper, inhabit the edges of ponds and streams, both foraging and interacting with conspecifics on the water surface. When at rest on the water surface, the weight of *D. triton* is typically distributed among the eight legs and the body. The downward pressure on the water surface distorts the surface, producing a dimple associated with each leg and with the body (Fig. 1). The spiders propel themselves across the water surface by rowing or by galloping. For rowing, they use the middle two pairs of legs (legs II and III) to develop thrust, a propulsive mechanism now characterized in detail (Suter et al., 1997). At the start of rowing locomotion, the propulsive legs are swung forward and pushed down into the water surface, resulting in more of the spider's weight being borne by the now deeper dimples associated with these propulsive legs. These legs are then swung backwards in turn (legs III followed by legs II), and it is each leg-cum-dimple that produces thrust, in the form of drag, and allows forward propulsion (Suter et al., 1997). The thrust phase of rowing is followed by a recovery phase during which the spider's weight is supported by contact between the water and the non-propulsive legs and the body and during which the propulsive legs return anteriad in preparation for the next thrust phase. This rowing locomotion (see also McAlister, 1959; Shultz, 1987) is distinct from the galloping locomotion used by these spiders during some kinds of prey capture (Gorb and Barth, 1994) and during escape from predators (R. B. Suter, unpublished data). For galloping, the spiders use the first three pairs of legs synchronously. During the thrust phase, the six propulsive legs are swept downwards and backwards, with their distal portions submerged. During the aerial phase, the spider has little or no contact with the water surface (the tips of legs IV are sometimes in contact) and the propulsive legs return anteriad in preparation for the next thrust phase (Gorb and Barth, 1994). Both the active aquatic gaits are distinct from the alternating tetrapod locomotion used on a solid substratum (Barnes and Barth, 1991; Shultz, 1987) and from passive sailing methods of locomotion (elevated legs I, Deshefy, 1981; stilting, Suter, 1999).

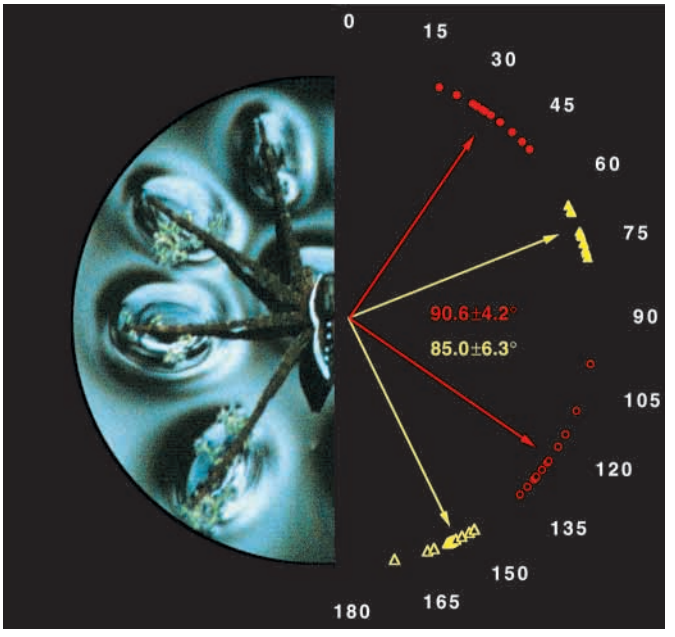


Fig. 1. Top view (left) of *Dolomedes triton* at rest on the surface of a pond. The legs and body of the spider distort the water surface, producing dimples under each leg end and under the body. During rowing (right), legs III (yellow symbols and arrows) begin the power stroke at 67.9±5.5° (filled symbols), end it at 153.0±9.8° (open symbols) and sweep through 85.0±6.3° (means ±1 angular deviation); legs II (red symbols and arrows), starting slightly later, begin the power stroke at 34.0±7.5°, end it at 124.7±9.5° and sweep through 90.6±4.2°. Individual values from 11 steps for one spider are shown (circles and triangles).

In the present study, we sought to determine whether there are limitations to the rowing gait that could explain the spider's use of the galloping gait when high speed is necessary. We evaluated three alternative (but not mutually exclusive) hypotheses: (1) because of anatomical and physiological limitations, a spider sweeping its propulsive legs backwards during rowing cannot achieve leg-tip velocities as high as those achieved during the downward and backward motion of the legs during galloping; (2) during rowing, the velocity attained during the thrust phase is lost during the drag-based deceleration of the recovery phase, a loss not experienced during galloping; (3) the properties of the substratum (e.g. the water's density, surface tension, deformability) influence the integrity of the dimples used during rowing and, as a consequence, limit the spider's ability to row at high velocities, a limitation not experienced during galloping because galloping locomotion does not depend upon dimples.

We evaluated both the anatomical limitation hypothesis (1) and the drag-during-recovery hypothesis (2) by studying the kinematics of rowing and galloping in intact spiders as revealed through high-speed videography. To evaluate the dimple integrity hypothesis (3), we measured horizontal and vertical forces on isolated leg segments under both static and non-turbulent flow conditions.

## Materials and methods

### *Spiders*

The subjects for these experiments, *Dolomedes triton* (Walkenaer) (Araneae, Pisauridae), were collected from small

ponds in Mississippi and were held in our laboratory under conditions described elsewhere (Suter et al., 1997).

### *Analyses of the rowing gait*

#### *Kinematics of rowing*

Because our methods for studying the kinematics of *D. triton* are given in detail in Suter et al. (1997), only an abbreviated version is given here. We videotaped 32 intact spiders of a range of instars in an arena that had a white bottom and clear plastic sides, filled to a depth of approximately 1 cm with distilled water. In a trial, we placed the test spider in the arena and recorded its movements from above using a high-speed video system (Kodak model EktaPro EM-1000) at 1000 images $s^{-1}$. The images were stored in S-VHS format (Sony, model 9500 MDR). For analysis, we used sequences of images in which the spider's initial velocity was between 0 and 0.02 m $s^{-1}$ (the spider was either at rest or was near the end of the recovery stroke from a previous rowing stroke) and the spider moved approximately in a straight line. We analysed the spider's motion in the horizontal plane by displaying each digitally paused video frame on top of a computer-generated *x,y* cursor grid (National Institutes of Health software Image, version 1.55 f) by means of a video scan convertor (Digital Vision, Incorporated, model TelevEyes/Pro, connected to an Apple Corporation Power Macintosh 7100/80AV). We manually digitized the coordinates of the anterior or posterior tip of the body every 5 ms for the duration of a propulsion episode and used the coordinates to calculate the displacement of the spider through time; velocity was calculated for each 5 ms interval; accelerations and decelerations were calculated as the slopes of the linear fits of three-point running averages of velocity as a function of time (Suter et al., 1997).

Using the same images and digital image-analysis software, we measured the angles of the legs relative to the long axis of the body, the angular velocity (ω, degrees $ms^{-1}$) of the propulsive legs (II and III) during the power portion of the rowing stroke and the lengths of the propulsive legs. We used the angular velocity and leg length to calculate the velocity of the leg relative to the cephalothorax at known distances from the leg's attachment to the spider. We used the lengths of legs II and III and spider mass to develop a regression model relating the two variables. In calculating mean angles and angular deviations, we followed circular statistical procedures described in Batschelet (1981).

#### *Measurement of horizontal thrust forces involved in rowing*

To make force measurements and to evaluate the integrity of dimples (see below), we used leg segments from killed adults. The leg segments were stored in dry air prior to attachment to the force balance; we used only the distal portions (tarsus plus part of tibia) of legs II and III, varying in length from 12 to 17 mm and tapering from a diameter of approximately 1.5 mm at the proximal end to 0.5 mm at the distal end. All observations and experiments were conducted at laboratory temperatures between 20 and 23 °C.

We used a horizontal balance to which a leg segment was attached (Suter et al., 1997) to measure forces on the leg segment in the horizontal plane. The balance employed an electronic clinometer (Applied Geomechanics Inc., model 900, biaxial clinometer) with a resolution of 0.01 ° ($1.75\times10^{-4}$ rad) to measure small angular displacements that were directly proportional to the horizontal force applied to the leg segment. In the experiments reported here, the leg segment was attached directly to the lower end of the vertical arm of the balance (Fig. 2) so that the depth of the leg segment (*d*) relative to the level of the water surface could be controlled.

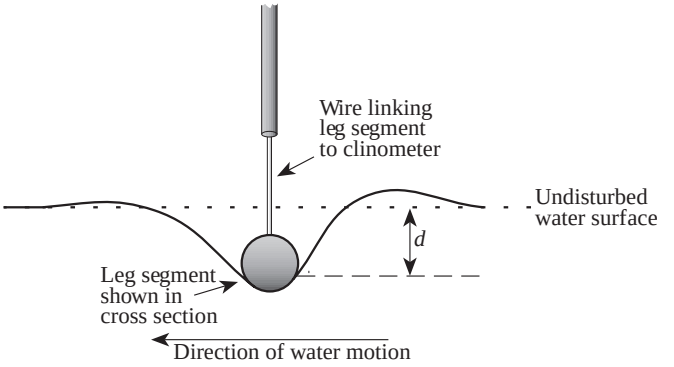


Fig. 2. Relationship between a leg segment and the water surface during measurements of horizontal forces ($F_{surf}$ and $F_{subm}$), showing dimple depth (*d*).

We propelled distilled water past the leg segment using a rotating flow tank that produced no detectable flow disturbance (Suter et al., 1997). In that respect, the relationship between the stationary leg and the moving but undisturbed water was the equivalent of the relationship between the relatively stationary water of a pond and the moving leg of a spider propelling itself across the pond surface.

Clinometer output (in volts) was digitized by an analog-to-digital (A/D) convertor (National Instruments Corporation, model NB-MIO-16L) driven by a custom-designed program (National Instruments software LabView 3) on a microcomputer (Apple Corporation Power Macintosh 7100/80AV). An infrared tachometer sensed turntable motion and conveyed that information, in the form of a series of voltage peaks, to the A/D convertor. The software program converted the clinometer's voltage into horizontal force (mN), *F*, and calculated the relative velocity (m $s^{-1}$) of the water, *U*, past the leg segment, which was located approximately 22 cm from the center of the rotating flow tank. For each experiment, consisting of a given leg length, *L*, and dimple depth, *d*, scatterplots of force as a function of water velocity were fitted with power curves (CA-CricketGraph software III v. 1.5.3), since we anticipated that total horizontal force, $F_t$, would be proportional to $U^{1.6}$ (Suter et al., 1997). The close agreement between the data and expectations from hydrodynamic theory for forces acting on a leg segment with associated dimple was discussed in Suter et al. (1997).

For the present study, we also needed to calculate expected values for forces acting on a submerged leg, both because the disintegration of a dimple results in a submerged leg segment

and because rapidly moving submerged leg segments provide thrust during galloping (see below). We used Denny's (1993) equations for Reynolds numbers (*Re*, equation 7.2 in Denny, 1993) and for drag coefficients ($C_d$, equation 7.10 in Denny, 1993) to calculate the drag force on a submerged cylinder (equation 4.29 in Denny, 1993):

$$F_{subm} = 0.5\rho_f U^2 A_f C_d , \quad (1)$$

where $\rho_f$ is the density of distilled water, $U$ is the horizontal velocity of the water flowing perpendicular to the long axis of the cylindrical leg segment, $A_f$ is the frontal area of one curved face of the leg and $C_d$ is the drag coefficient. For these calculations, we restricted $U$ to between 0.01 and 0.5 m s$^{-1}$; in this velocity range, *Re* varied over the range 10–500 and $C_d$ varied over the range 4.242–0.705. In these calculations, we ignored the acceleration reaction and other unsteady mechanisms because we had previously demonstrated (Suter et al., 1997) that both the angular velocity of the legs and the velocity of the leg tips were constant during rowing.

*Evaluation of dimple integrity during rowing*

The leg-cum-dimple (Figs 1, 2) is the structure that encounters drag and thereby produces thrust as it moves through the water during rowing (Suter et al., 1997). To investigate the integrity of this structure under the conditions encountered during rowing, we measured the total horizontal force ($F_t$) on a leg-cum-dimple at constant velocity ($U$) while slowly increasing dimple depth ($d$) and looked for an abrupt decrease in $F_t$ coincident with the disappearance of the dimple (and submersion of the leg segment) that was apparent on visual inspection. We repeated this process at a variety of velocities, allowing us to visualize and quantify the disintegration of the dimple and the changes in $F_t$ as functions of both $U$ and $d$.

*Measurement of vertical forces supporting spiders on the water surface*

To measure the upward force on an object pushed downwards onto the water surface, we mounted either a segment of spider leg (long axis horizontal, length 12 mm) or a flat disk (plane of disk parallel to water surface, diameter 2.5–6 mm) coated with petroleum jelly onto the end of a needle probe attached to a micromanipulator. Motion of the micromanipulator pushed each disk or the leg segment downwards onto the surface of distilled water contained in a Petri dish that rested on the pan of an electronic balance (Sartorius, model R-200-D, precision to $10^{-5}$ g). Once the test item was in contact with the water, measured increments of downward motion of the test item resulted in increases in balance readings until the test item submerged. We used both a leg segment and disks in these measurements to confirm that the circumference (Denny, 1993; Vogel, 1994), rather than the area, of the object was the relevant variable.

During rowing, the distal parts of the spider's legs are initially parallel to the water surface but, during the power stroke, they are pushed down below the level of the undisturbed surface. When in this position, the distal parts of the legs are no longer parallel to the water surface. Because the upward force on a leg segment is a function of the perimeter of the leg–water interface, we needed to be able to estimate the length of that interface. We did not directly measure the perimeter ($p$) of the rectangular leg–water interface of experimental leg segments mounted horizontally or of the nearly elliptical leg–water interface of segments mounted at an angle to the surface. Instead, we treated all such perimeters as being rectangular and estimated $p$ as twice the length of the segment that actually contacted the water plus twice the average width of the segment.

*Analyses of the galloping gait*

The present study concerns limitations on rowing rather than the details of propulsion during galloping. Consequently, we have included here only those aspects of galloping that contribute to an understanding, by comparison, of the limitations of rowing.

*Kinematics of galloping*

Our analysis of galloping had two phases: first, we used the videographic techniques outlined above to measure horizontal velocities for comparison with the velocities attained by rowing spiders; second, we used a more elaborate arena to study galloping kinematics in detail.

In contrast to rowing, in which the motion is in or very near the plane of the water surface, galloping is much more three-dimensional and so cannot be adequately videotaped from a single angle. To study galloping, we placed a spider in a 38 l glass aquarium filled to a depth of 8 cm. We placed a 7 cm×25 cm mirror under water in the center of the aquarium with its long axis parallel to the long axis of the aquarium. The mirror was mounted at 45° from the vertical so that, when videotaped through the long side of the aquarium, it presented a view looking up through the surface of the water. The central axis of the video camera's lens ran horizontally through the center of the mirror so that a recording showed both the ventral surface of the spider as it passed above the mirror and an oblique view (at approximately 5°) of the underside of the water surface. To analyze galloping, we used the same high-speed videographic and digitization equipment and techniques as described above for the analysis of rowing. We analyzed only leg strokes that were perpendicular to the axis of the camera lens. From the oblique view, as seen in video images, we recorded the length of the leg segment that was below the level of the undisturbed water surface, the coordinates of its distal tip, the coordinates of the intersection of the leg with the water surface and the angle formed between the submerged leg segment and the water surface. From the reflected part of a video image, we recorded a spider's horizontal velocity and the angular velocity (in the horizontal plane) of the femur of the leg from which we had recorded subsurface kinematics. For this paper, we made a detailed analysis of six galloping strokes from a single female spider with a mass (0.289 g, 2.83 mN) nearly identical to the mean mass of the spiders analyzed in our rowing kinematic studies.

*Calculation of horizontal and vertical thrust forces involved in galloping*

Analyses of the kinematics of galloping gave us information about the dynamics of the subsurface portion of the leg. We assumed that, although the subsurface portion of the leg was not entirely surrounded by water, its motion through the water created a drag force identical to that created by a fully submerged leg segment of the same length and moving at the same average velocity; this is a plausible assumption because the drag on a submerged cylinder (equation 4.29 in Denny, 1993; equation 1, this paper) is proportional to the frontal surface area ($A_f$). We then calculated the total thrust force exerted by that leg segment, using equation 1, in a direction perpendicular to the leg's long axis, and used trigonometry to resolve that vector into its horizontal and vertical components. A further assumption of these calculations, that unsteady aspects of force production (Daniel, 1984) were negligible, was not supported by the data (see below).

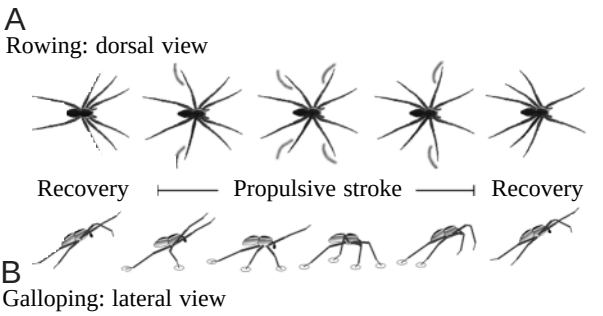


Fig. 4. Video images showing a single stroke cycle for rowing (A) and galloping (B). Rowing involves the use of legs III and II to generate thrust, and sequential propulsive strokes are linked by recovery intervals during which the spider's forward motion is slowed by drag between the spider and the water. During galloping (the legs on the spider's left are not shown), the anterior three pairs of legs generate thrust, and sequential propulsive strokes are linked by recovery intervals during which the spider is airborne; ellipses indicate contact with the water, with leg tips submerged.

## Results

Videographic measurements made on 32 spiders (mass 0.28±0.20 g, mean ± S.D.) indicated a non-overlapping distribution of sustained velocities between rowing spiders (0.03–0.21 m s$^{-1}$) and galloping spiders (0.28–0.72 m s$^{-1}$) (Fig. 3). Our analyses confirmed that the two gaits are qualitatively distinct and quantitatively discontinuous. We have first analyzed the two gaits separately and then made explicit comparisons.

### *Analyses of the rowing gait*

*Kinematics of rowing: data from high-speed videography*

During rowing (Fig. 4A), the spider was always in contact with the water surface and used its third and second pairs of legs in that order (III–II); for each leg, the spider first depressed the water surface by pushing downwards with the distal part of the leg and then swept the leg posteriad; throughout the backward sweep, the leg remained relatively straight, and at the middle of the stroke a line between the tarsus (the leg's most distal segment) and the coxa (the most proximal segment) formed an angle of less than 10° with the horizontal (see also Suter et al., 1997; Shultz, 1987). Despite the relatively low sustained velocities recorded during rowing (Fig. 3), higher peak intermittent velocities (0.12–0.56 m s$^{-1}$) were reached by rowing spiders at the end of the power phase of a rowing stroke. The peak velocities were not sustained, however, because rowing spiders decelerated rapidly (Fig. 5A) between power strokes. The net forces causing decelerations were usually smaller in magnitude than the forces causing the accelerations achieved in the power phase (Table 1); these forces varied with spider mass (Fig. 6).

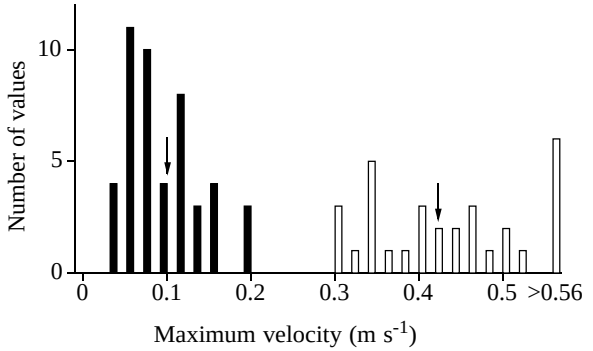


Fig. 3. Frequency distribution of sustained horizontal velocities ($U$) during spider locomotion on the water surface. The rowing gait (filled columns) always occurred at $U$<0.22 m s$^{-1}$, whereas the galloping gait (open columns) occurred at $U$>0.27 m s$^{-1}$. Medians for the two distributions are indicated by arrows.

Leg length ($L$, mm) and leg angular velocity (ω, degrees ms$^{-1}$) varied as functions of spider mass ($M$, g) (Fig. 7):

$$L = 13.22\log_{10}M + 28.73 \ (r^2=0.94, P<0.01), \quad (2)$$

$$\log_{10}\omega = -0.328\log_{10}M - 0.256 \ (r^2=0.38, P<0.01). \quad (3)$$

Stride frequency (strides s$^{-1}$) also varied with mass ($\propto M^{-0.36}$), as expected from theoretical considerations (Hill, 1950).

During a rowing stroke, spiders swept each of their propulsive legs through approximately 90° in the horizontal plane, legs III beginning each sweep at approximately 68° and legs II beginning each sweep at approximately 34° (Fig. 1).

*Horizontal thrust forces involved in rowing: data from leg segments in flowing water*

The force generated by water moving past a horizontal leg segment varies both with the velocity of the water and with the depth of the dimple formed by the leg segment pressing down into the water (Suter et al., 1997). In the present study, the relationship between force and velocity was well described ($r^2$>0.98) by a family of power functions (Fig. 8A) in which the exponents did not vary significantly with dimple depth but the coefficients increased significantly and linearly with

Table 1. *Measured accelerations during the power phases and decelerations during the glide phases of rowing strokes of a 0.308 g spider*

| Stroke acceleration ($m\,s^{-2}$) | $N$ | $r^2$ | $F_{surf}$, calculated force (mN) | Glide acceleration ($m\,s^{-2}$) | $N$ | $r^2$ | $F_{surf}$, calculated force (mN) |
|---|---|---|---|---|---|---|---|
| 1.232 | 7 | 0.832 | 0.379 | –1.767 | 8 | 0.923 | –0.544 |
| 0.983 | 9 | 0.947 | 0.303 | –0.476 | 17 | 0.946 | –0.147 |
| 2.347 | 10 | 0.975 | 0.723 | –0.704 | 13 | 0.969 | –0.217 |
| 1.414 | 6 | 0.918 | 0.436 | –0.735 | 5 | 0.982 | –0.226 |
| 2.328 | 11 | 0.931 | 0.717 | –1.011 | 13 | 0.947 | –0.311 |

$F_{surf}$, the horizontal force produced by a leg on the surface, was calculated using Newton's second law.

increasing depth (Fig. 8B). Accordingly, we used the mean value of the exponents (1.686) and the linear equation relating the coefficient ($c$) to the dimple depth ($d$, mm):

$$c = 3.032d + 2.891\,, \tag{4}$$

to describe the horizontal force ($F_{surf}$) generated by water flowing at velocity, $U$, acting on a leg segment ($L$=14.5 mm) bearing a dimple:

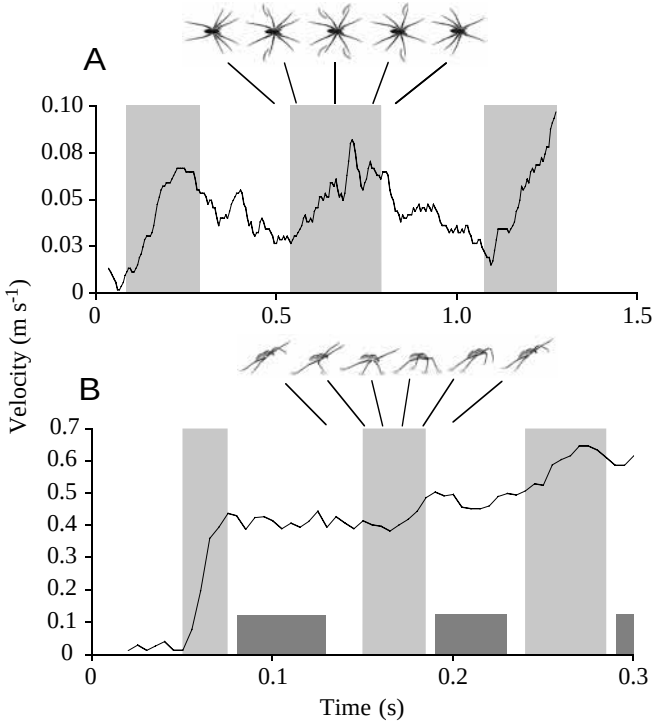


Fig. 5. Changes in velocity over time for (A) rowing and (B) galloping spiders. The images above the graphs show the positions of the legs at corresponding points in the graphs. Rowing spiders (A) accelerate during the power sweep of legs II and III (light tinted regions) and decelerate during the glide phase of rowing locomotion when they provide no forward thrust but do experience backward drag (see Table 1). Galloping spiders (B) accelerate rapidly during the first of several power strokes, but only slightly during later power strokes (shaded regions) and do not decelerate measurably between power strokes. For most of the time between power strokes, a galloping spider is fully air-borne (dark tinted regions).

$$F_{surf} = cU^{1.686}\,. \tag{5}$$

Because this relationship is based on data from a 14.5 mm leg segment and because $F_{surf}$ is directly proportional to frontal area (for a leg-cum-dimple, the product of $L$ and $d$; Suter et al., 1997), a more general expression that combines equations 4 and 5 and accounts for $L$ is:

$$F_{surf} = \frac{(3.032d + 2.891)U^{1.686}L}{14.5}\,. \tag{6}$$

The force generated by water moving past a submerged horizontal leg segment varied with the velocity of the water but not with depth, because of the absence of a dimple. Our measurements (Fig. 9) showed that the relationship between force ($F_{subm}$) and velocity ($U$) for a submerged leg segment oriented perpendicular to the flow (corrected for leg length as in equation 6 because, again, drag is directly proportional to frontal area; Denny, 1993; Vogel, 1994) was:

$$F_{subm} = \frac{3.865U^{1.600}L}{14.5}\,. \tag{7}$$

This relationship closely matches our expectations derived from calculations based on hydrodynamic theory (equation 1) over the range of velocities tested (Fig. 9).

*Dimple integrity during rowing*

In still water, the maximum depth ($d_{max}$) of a dimple associated with a leg segment was a function of the perimeter of the leg segment ($p$) where it interacted with the water surface (Fig. 10). For an approximately cylindrical spider leg, the perimeter is circular (and at a minimum) when the leg pushes into the water vertically. As the angle of the leg relative to horizontal moved away from 90 °, the perimeter became an increasingly elongated ellipse for which the perimeter was maximized at 0 °. In practice, the relationship between $d_{max}$ and the perimeter ($p$) of the leg segment was logarithmic:

$$d_{max} = 0.918\log_{10}p + 2.367\,, \tag{8}$$

over the range 3–32 mm (Fig. 10B) and never rose above 3.8 mm.

In flowing water, $d_{max}$ depended both on the perimeter and on the velocity of flow ($U$). Under experimental conditions, as

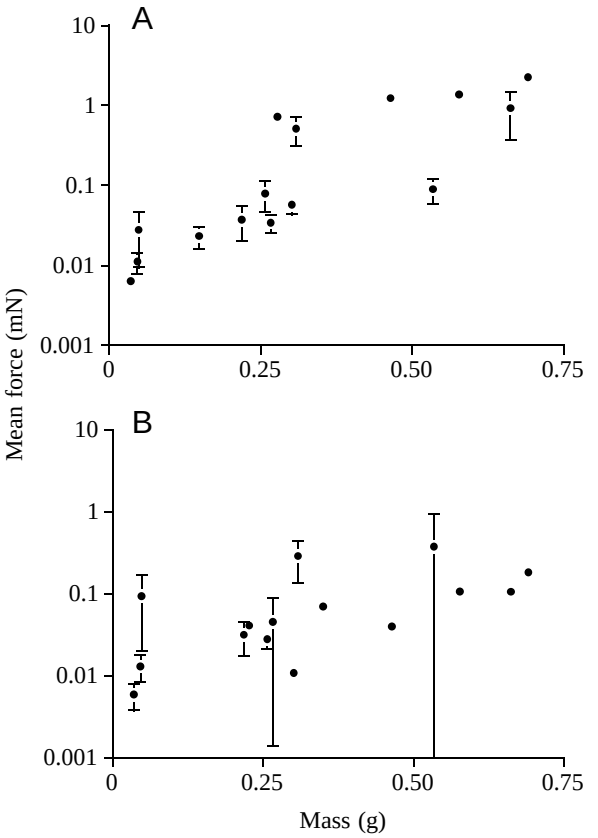


Fig. 6. Forces that accelerate and decelerate a spider during rowing vary with spider mass. During the propulsive phase of a rowing stroke (A), spiders are accelerated by thrust forces that increase with spider mass (note logarithmic force scale). During the recovery phase (B), which is of approximately the same duration as the propulsive phase (see Fig. 5A), spiders are decelerated by drag forces that also increase with spider mass. Because these forces are similar in magnitude for spiders of a given mass, much of the acceleration achieved during the propulsive phase is cancelled during the recovery phase (see Fig. 5A). Values are means ± S.D., $N$=15. The large standard deviations in B indicate substantial variation in the forces acting on some spiders during recovery, variation that is attributable in part to postural adjustments by the spiders (R. B. Suter, unpublished data).

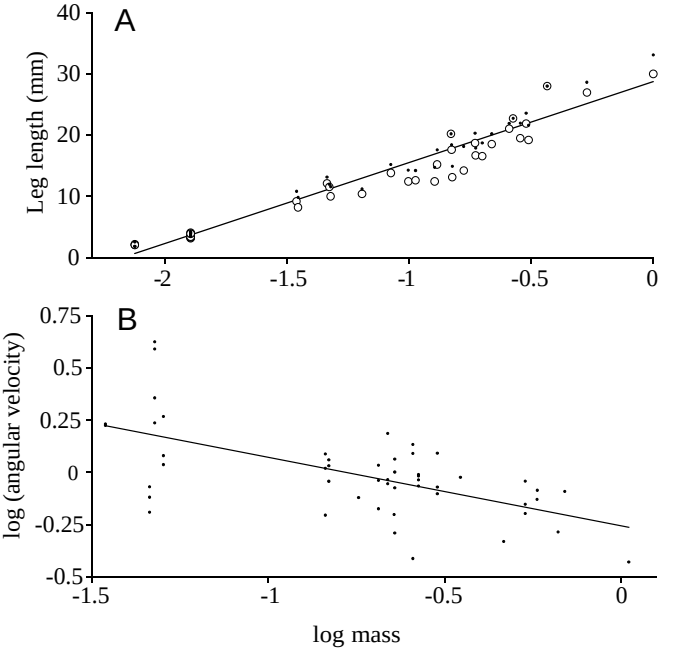


Fig. 7. (A) The allometric, semi-logarithmic relationship between spider mass (g) and leg length (mm); points representing legs II (●) were pooled with those representing legs III (○), and a linear fit to the pooled data resulted in equation 2. (B) The allometric, double-logarithmic relationship between spider mass and the angular velocity of propulsive legs (legs III) (degrees ms$^{-1}$); a linear fit to the data yielded equation 3.

we increased dimple depth ($d$) at constant $U$, exceeding $d_{max}$ resulted in disintegration of the dimple and submersion of the leg segment, with a consequent diminution of the force applied to the leg segment (Fig. 11A). The depth at which this disintegration occurred decreased linearly with increasing velocity (Fig. 11B) as:

$$d_{max} = -7.933U + 4.095 \ (r^2=0.99, P<0.01)\,. \quad (9)$$

To define the variable $y$-intercept, we combined the two equations to give $d_{max}$ as a function of both $U$ and $p$:

$$d_{max} = -7.933U + 0.918\log_{10}p + 2.367\,. \quad (10)$$

We assumed, in combining the two equations, that there was no multiplicative interaction between $p$ and $U$, and we have, as yet, no empirical way of testing that assumption.

Equation 10 describes a curved surface on which $d_{max}$ decreases as $U$ increases and as $p$ decreases. Because $d_{max}$ defines the boundary condition at which a rowing spider's propulsive leg switches from dimple-bearing to submerged, it also defines the condition at which the force generated by the leg (or by water moving past a stationary leg segment) switches from $F_{surf}$ to $F_{subm}$. The force that can be generated by a single propulsive leg is therefore described by a surface containing a discontinuity at $d_{max}$ (Fig. 12).

*Vertical forces supporting spiders on the water surface*

As a hydrophobic structure is pushed downwards onto water, its progress is resisted by buoyant forces (proportional to the amount of water displaced) and by surface tension (proportional to the amount of new water surface formed) (Denny, 1993). For the small objects tested here (circular disks coated with petroleum jelly and a 12 mm long leg segment), the relationship between dimple depth ($d$) and vertical force per unit of perimeter ($F_{vert}$) was linear (Fig. 13). We chose to use the relationship derived from the leg segment:

$$F_{vert} = 0.032d + 0.005\,, \quad (11)$$

because of its closer connection to the natural situation we were seeking to understand.

A consequence of the vertical resistance force experienced by a spider's leg as the leg is pushed downwards is that the maximum depth of the dimple that accompanies the leg is

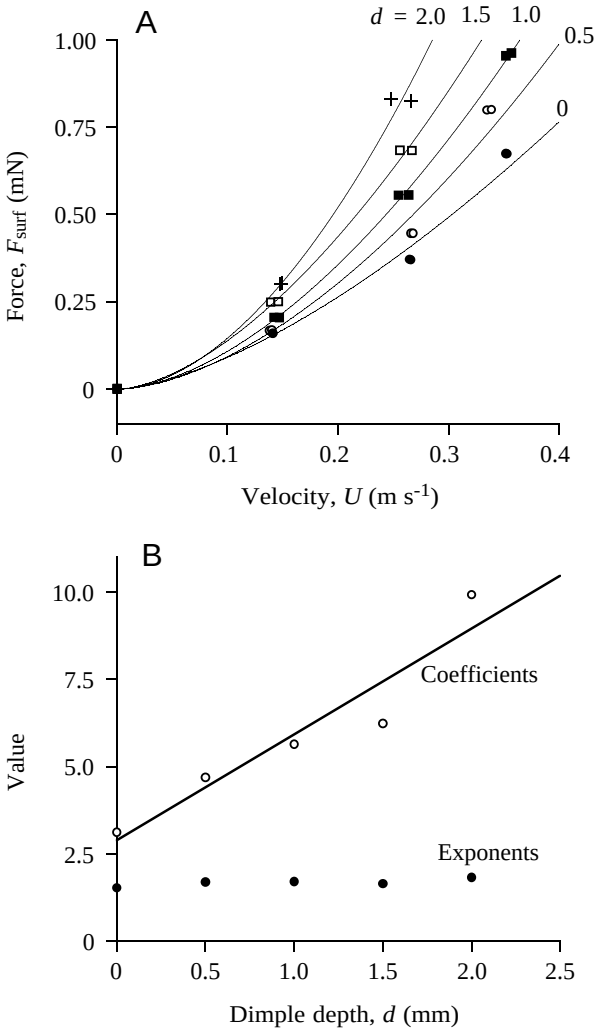


Fig. 8. (A) The horizontal force ($F_{surf}$) generated by water flowing past a 14.5 mm long leg segment and its accompanying dimple is a power function of water velocity ($U$) and is strongly influenced by dimple depth ($d$). Equations for power functions, in order of descending $d$: $F_{surf}=9.93U^{1.83}$, $r^2=0.991$; $F_{surf}=6.24U^{1.65}$, $r^2=0.995$; $F_{surf}=5.64U^{1.71}$, $r^2=0.998$; $F_{surf}=4.69U^{1.70}$, $r^2=0.985$; $F_{surf}=3.12U^{1.53}$, $r^2=0.986$. (B) The influence of $d$ on the coefficients and exponents of the power functions. The regression line is significant for the coefficients ($F$=26.51, $P$=0.014) (equation 4), but not for the exponents ($F$=5.37, $P$=0.103).

dependent upon the weight of the spider and the distribution of that weight among the legs and the body. Typically, at the beginning of a rowing stroke, a spider shifts its weight from being approximately evenly distributed among its eight legs and its body (Fig. 1) to being increasingly concentrated over the distal third of each of the propulsive legs (legs II and III). This shift can mean that nearly all the spider's weight is borne by a relatively small total length of leg, and the dimples formed thereby must be proportionately deeper if vertical support is to be sufficient (Table 2).

The analysis demonstrated that changes in the orientation (in a vertical plane) of the propulsive part of a leg affected the achievable $F_{surf}$ minimally (e.g. 1.498 mN *versus* 1.503 mN; for four legs) and that, although the number of legs used in rowing strongly influenced $d_{max}$, the number of legs used had a relatively minor influence on achievable $F_{surf}$ (Table 3). Our exploration of this situation (Tables 2, 3) showed that, for a 0.28 g spider (the mean mass of live spiders used in this study) rowing with four legs, $d_{max}$ for a relatively horizontal leg was 1.06 mm (average depth for the inclined leg) and the

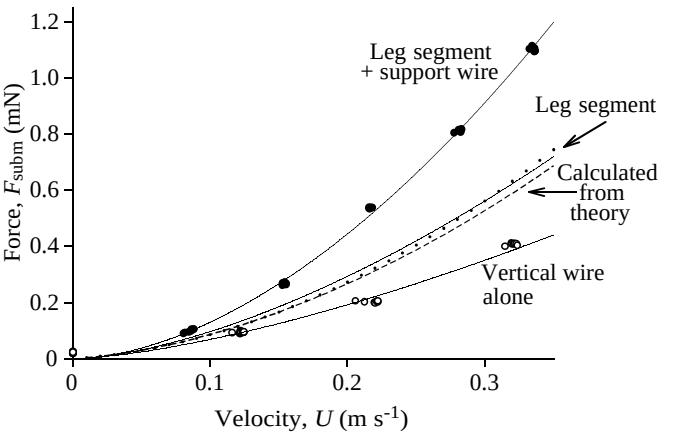


Fig. 9. Horizontal force ($F_{subm}$) generated by water flowing around a submerged 14.5 mm long leg segment as a function of water velocity $U$ (●), calculated as the difference between forces on the segment with its support wire ($F_{subm}=7.703U^{1.771}$, $r^2=0.999$, $N$=47) and those on the support wire alone ($F_{subm}=2.089U^{1.481}$, $r^2=0.990$, $N$=25). A power fit (middle solid line; $F_{subm}=3.865U^{1.600}$, $r^2=0.994$) to the calculated $F_{subm}$ is in accordance with theoretical expectations (using equation 1; dashed line).

Table 2. *Calculated vertical (upward) and horizontal forces on a leg (inclined at 17 °) from a 0.28 g (2.74 mN) spider*

| Segment of leg | Proportion of distance to leg tip | Dimple depth (mm) | Peri-meter (mm) | Vertical force (mN) | Horizontal force (mN) |
|---|---|---|---|---|---|
| 1 | 0.6630 | 0 | 2.72 | 0 | 0 |
| 2 | 0.6984 | 0.235 | 2.72 | 0.0341 | 0.0188 |
| 3 | 0.7339 | 0.470 | 1.52 | 0.0305 | 0.0237 |
| 4 | 0.7694 | 0.705 | 1.52 | 0.0419 | 0.0289 |
| 5 | 0.8049 | 0.940 | 1.52 | 0.0533 | 0.0345 |
| 6 | 0.8403 | 1.175 | 1.52 | 0.0648 | 0.0405 |
| 7 | 0.8758 | 1.410 | 1.52 | 0.0762 | 0.0469 |
| 8 | 0.9113 | 1.645 | 1.52 | 0.0876 | 0.0536 |
| 9 | 0.9468 | 1.880 | 1.52 | 0.0990 | 0.0607 |
| 10 | 0.9823 | 2.115 | 2.72 | 0.1977 | 0.0682 |
| Total force generated by one leg | | | | 0.6850 | 0.3758 |

Each segment, as arbitrarily defined, had a length equal to one-tenth of the length of the distal third of the leg. Segments are numbered beginning at the proximal end of the distal third of the leg.

For these calculations, both leg length ($L$) and leg-tip velocity ($U$) were allometrically scaled to spider mass using equations 2 and 3, respectively ($L$=21.4 mm; $U$=0.315 m s$^{-1}$).

Vertical force was calculated using equation 11; horizontal force was calculated using equation 6.

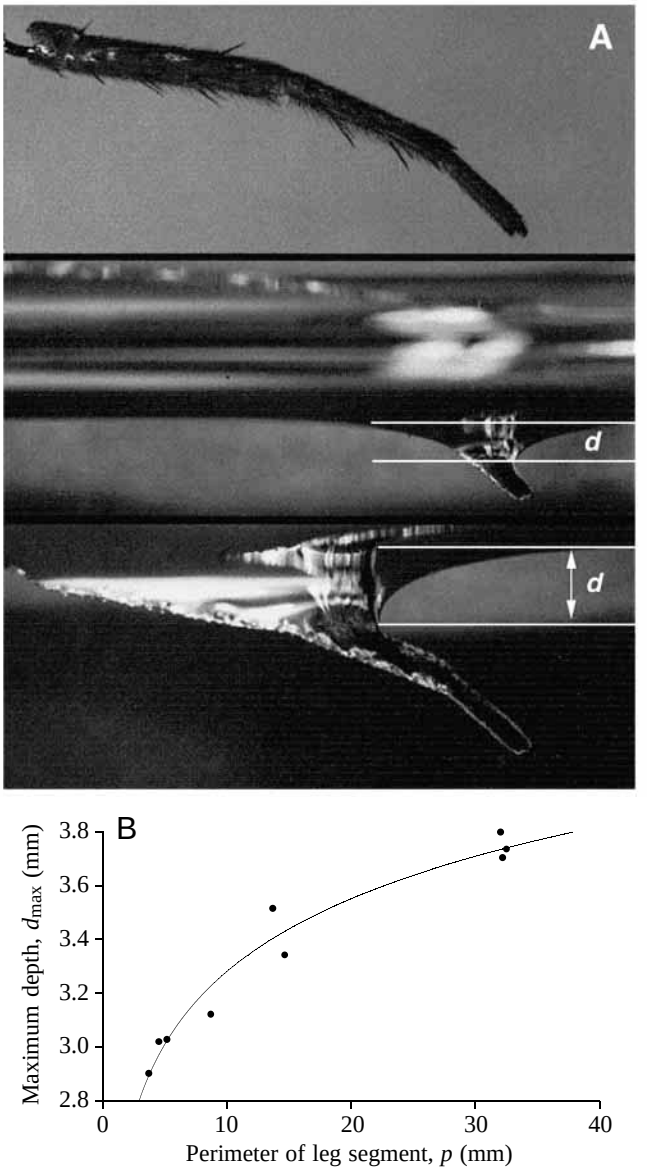


Fig. 10. (A) The distal third of a *Dolomedes triton* leg in air (top), pushed slightly below the undisturbed water surface (middle) and pushed still further below the surface (bottom). The vertical distance between the undisturbed water surface and the interface between the water surface and the leg is the dimple depth, *d*. (B) At water velocity $U$=0, dimples are stable, and maximum dimple depth ($d_{max}$) varies with the length (perimeter) of the leg–water interface ($p$), a relationship that is well described by a logarithmic curve fit ($d_{max}$=0.918log$_{10}p$+2.367; $r^2$=0.961).

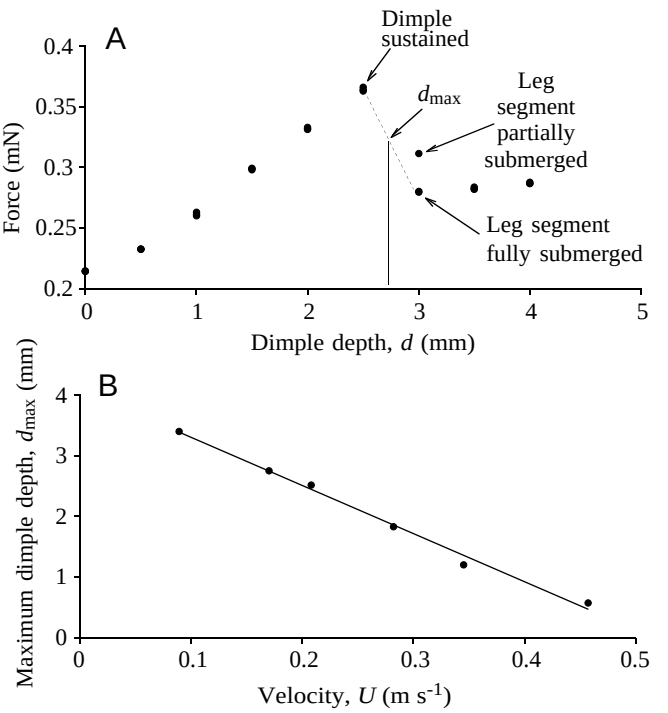


Fig. 11. (A) Disintegration of the dimple defines the discontinuity between the horizontal force for a leg at the surface, $F_{surf}$, and the horizontal force for a submerged leg, $F_{subm}$, for a horizontal leg segment (length $L$=17 mm) in water flowing at a velocity, $U$, of 0.17 m s$^{-1}$. The depth at which disintegration occurs ($d_{max}$) is taken at the midpoint between the dimple-sustaining and submerged depths. At each value of $d$, force is represented by three data points (measured at intervals of 2 s); the value for the partially submerged leg segment was the first (in time) of the three points for $d$=3 mm, a time at which the dimple was still intact along part of the leg segment. (B) Maximum dimple depth ($d_{max}$) varies linearly with $U$ (see equations 9, 10).

corresponding maximum $F_{surf}$ was 0.376 mN per propulsive leg (Table 2). Note, however, that most of the values of $F_{surf}$ reported in Table 3 could not actually be attained *in vivo* because they require dimple depths or leg-tip velocities at which dimples cannot exist.

Using the inclined leg as our standard (Table 2), we calculated that a 0.48 g spider, pressing down to the maximum $d$=3.8 mm with the distal third of each of its four propulsive legs, could just support all its weight on those four appendages. Heavier spiders would have to support some of their weight on the water surface under the abdomen and cephalothorax or under the tips of non-propulsive legs.

*Synthesis of rowing results*

In the example of the 0.28 g spider we began exploring above, $d_{max}$ (constrained by spider weight) was 1.06 mm, but the leg-tip velocity used in the calculations, 0.315 m s$^{-1}$ (Table 3), would only constrain $d_{max}$ to less than 1.60 mm (Fig. 11B; equation 10). Therefore, for the 0.28 g spider, part of the $F_{surf}$ surface (Fig. 14A) would be inaccessible because of the low mass of the spider (Fig. 14B). (We recognize that the spider could increase its effective weight, and thereby increase $d_{max}$, momentarily by accelerating its limbs in the vertical plane while stroking the legs. However, we have seen no evidence of that tactic in our measurements of dimple depths, as reflected in shadows cast by the dimples, during rowing; R. B. Suter, unpublished data.) Moreover, we know that the mean leg-tip velocity for a *D. triton* of that mass was 0.315 m s$^{-1}$

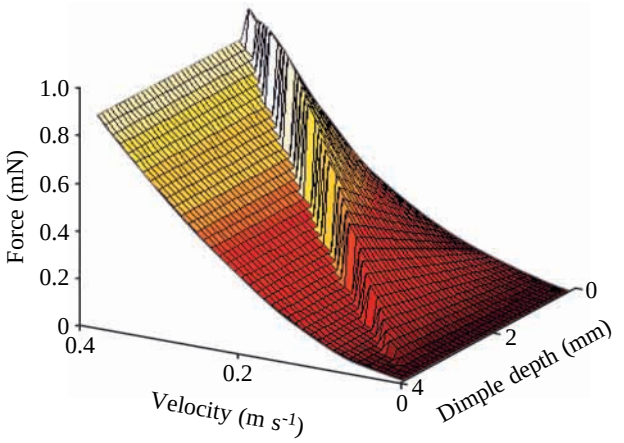


Fig. 12. The relationship between force, velocity and dimple depth. The horizontal force, $F_t$, on a 14.5 mm leg segment is a discontinuous function of $U$, the velocity of water flowing past the leg segment, and $d$, the depth of the dimple formed by the leg segment pressing down on the water surface, with the location of the discontinuity defined by $d_{max}$, the maximum depth at which a dimple can be maintained at each velocity. The surface to the right represents the horizontal force for a leg at the surface, $F_{surf}$, and the surface to the left represents the horizontal force for a submerged leg, $F_{subm}$. Color is tied to the value of $F_t$ (except at the discontinuity) such that lighter colors represent higher forces.

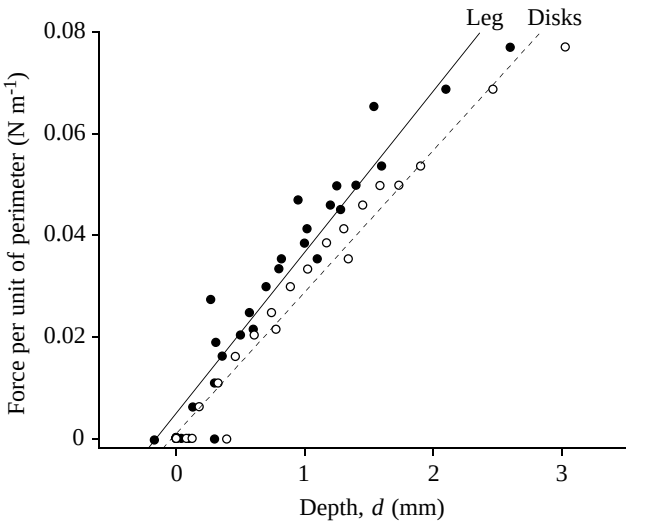


Fig. 13. The relationship between dimple depth, $d$, and the force per unit (mm) of perimeter ($F_{vert}$). Buoyancy and the vertical component of surface tension combine to push upwards on hydrophobic objects pushed downwards onto the water surface. The relationship is linear both for circular disks (●; $F_{vert}$=0.028$d$+0.001, $r^2$=0.968, $P$<0.01) and for a 12 mm leg segment (○; $F_{vert}$=0.032$d$+0.005, $r^2$=0.920, $P$<0.01). The linear fit for the leg segment was used (equation 11) in calculating maximum dimple depth, $d_{max}$.

(Fig. 7; equations 2 and 3) so, during an average rowing stroke, this 0.28 g spider also could not cross the discontinuity between $F_{surf}$ and $F_{subm}$; but during a more rapid rowing stroke, at a velocity greater than 0.315 m s$^{-1}$ (equation 2, extreme velocities in Fig. 7B), the maximum force generated by the leg segment would be further constrained by dimple disintegration at the discontinuity (Fig. 14B).

For a more massive spider (0.52 g, Table 3), the full range of possible dimple depths (0–3.8 mm, Fig. 10) could be used because, even rowing with all four propulsive legs, it would require dimples with $d$>4.0 mm to support the spider's mass on the distal third of the spider's four propulsive legs. Thus, the maximum dimple depth could be reached at low leg-tip velocities ($U$<0.037 m s$^{-1}$, equation 9), but at $U$=0.300 m s$^{-1}$, the average leg-tip velocity for spiders of that mass (equations 2 and 3), only dimples of $d$<1.18 mm could be maintained (Fig. 11B and equation 10; Fig. 14C,D).

Under the constraints outlined above, the maximum thrust available to a 0.28 g spider during rowing would be 1.498 mN (Table 2; four legs, 0.376 mN per leg; 100 % of the spider's weight supported by the four propulsive legs) and the maximum available to a 0.52 g spider would be 1.180 mN (only 34.5 % of

Table 3. *Effects of spider mass on the available range of dimple depths*

| Spider mass (g) | Mean leg-tip velocity (m s$^{-1}$) | Propulsion using the distal thirds of four legs | | Propulsion using the distal thirds of two legs | |
|---|---|---|---|---|---|
| | | $d_{max}$ (mm) | $F_{surf}$ (mN) | $d_{max}$ (mm) | $F_{surf}$ (mN) |
| 0.04 | 0.285 | 0.39 | 0.319 | 1.05 | 0.207 |
| 0.12 | 0.321 | 1.10 | 0.844 | **2.51** | **0.627** |
| 0.20 | 0.320 | **1.75** | **1.207** | **3.80** | **0.952** |
| 0.28 | 0.315 | **2.35** | **1.503** | **5.01** | **1.233** |
| 0.36 | 0.309 | **2.93** | **1.774** | **6.17** | **1.494** |
| 0.44 | 0.304 | **3.46** | **2.033** | **7.22** | **1.742** |
| 0.52 | 0.300 | **4.01** | **2.265** | **8.33** | **1.974** |

For heavier spiders, theoretically attainable maximum dimple depth, $d_{max}$, and horizontal force for a leg on the surface, $F_{surf}$, cannot be reached (values in bold type) because of perimeter and velocity constraints on $d_{max}$ (see Figs 10–12).

$d_{max}$ was calculated using equation 2; $F_{surf}$ was calculated using equation 3.

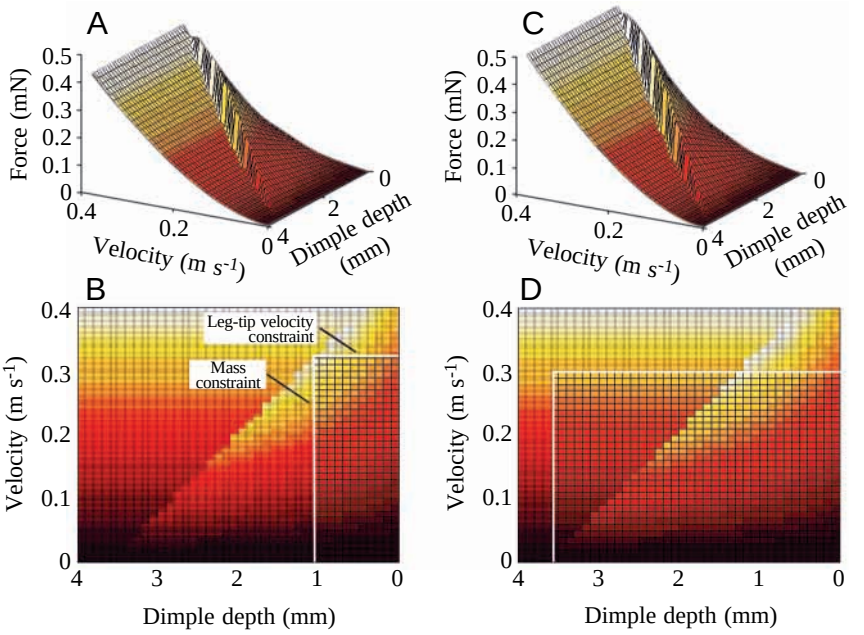


Fig. 14. Total horizontal force, $F_t$, on the leg segments of a 0.28 g spider (A) is constrained (B) by the spider's mass (*via* $d_{max}$, vertical line) and by leg-tip velocity (horizontal line) to the in-focus portion of the $F_{surf}$ surface. The $F_t$ of a 0.52 g spider (C), in contrast, is less constrained (D) by mass and more constrained by the disintegration of the dimple at the discontinuity defined by equation 10. See Fig. 12 for explanation of axes. $d_{max}$, maximum dimple depth; $F_{surf}$, the horizontal force for a leg at the surface.

the spider's weight supported). Because horizontal acceleration is constant during most of the power stroke of rowing (Suter et al., 1997), we used these force values to estimate maximum theoretical accelerations (neglecting opposing drag forces) for each of the spiders: 5.35 m s$^{-2}$ for the 0.28 g spider and 2.27 m s$^{-2}$ for the 0.52 g spider. Knowing that the propulsive legs sweep through approximately 88 ° during a power stroke (Fig. 1) and knowing average angular velocities for spiders of different sizes (equation 3), we calculated that these forces would be applied over periods of 0.105 s and 0.129 s respectively. The smaller spider, then, could theoretically reach a velocity of 0.56 m s$^{-1}$ at the end of a power stroke, but the larger spider could only reach 0.29 m s$^{-1}$. Neglecting opposing drag forces, however, is unrealistic: during a rowing stroke, spiders of all sizes had their anterior and posterior leg pairs in contact with the water surface (but not producing thrust) and, because the sweeps of legs III had only partial temporal overlap with the sweeps of legs II, the propulsive legs were also in non-propulsive contact with the water surface during part of the power stroke. In addition, for the larger spider, more than 65 % of its weight was borne by the water surface contacting its cephalothorax and abdomen throughout the power stroke. All these points of contact experienced drag that was proportional to $d$ and to $U^{1.686}$ (equation 6). Moreover, during the recovery phase between rowing power strokes, all the weight of a spider rested on the water surface, producing a net deceleration (Figs 5A, 6B; Table 1) that was again proportional to $d$ and to $U^{1.686}$.

Increases in stride frequency could also yield higher sustained rowing velocities, but velocities would again be constrained by dimple maintenance requirements: increased stride frequency cannot be attained without proportionally increased leg-tip velocity, and increasing leg-tip velocity threatens the integrity of the dimple unless its depth is decreased.

*Analyses of the galloping gait*

*Kinematics of galloping: data from high-speed videography*

During galloping (Fig. 4B), the spider was only intermittently in contact with the water and used the three anterior pairs of legs for propulsion, all moving pairwise in the same sequence as was used in rowing (III–II–I); for each leg, the spider pushed downwards and backwards and simultaneously flexed the leg at the femoral-patellar and patellar-tibial joints so that, at the middle of the stroke, a line between the tarsus and the coxa formed an angle of 30–70 ° with the horizontal (see also Gorb and Barth, 1994). Galloping spiders showed no detectable horizontal deceleration during the recovery phase of a propulsive stroke (Fig. 5B), a period during which the spiders were airborne.

Sequences of videographic images of the subsurface parts of propulsive legs showed that, during galloping, the legs were swept downwards and backwards through the water so rapidly that an air-filled cavity followed each throughout the propulsive phase. Typically, during a single propulsive stroke, the path followed by the subsurface leg tip was irregular (Fig. 15A–C), and the angular velocity of the subsurface parts of the leg (Fig. 15D–F) varied considerably between 1 degree ms$^{-1}$ and 8 degrees ms$^{-1}$. Maximum leg-tip velocities during these galloping power strokes varied from 0.71 to 1.20 m s$^{-1}$ (0.98±0.21 m s$^{-1}$, mean ± S.D., $N$=6).

Throughout each of the six galloping strokes analyzed here, the horizontal location (on the water surface) of the intersection between the leg and the water surface was nearly stationary: despite the rapid horizontal locomotion of the spider (velocity 0.53±0.17 m s$^{-1}$, mean ± S.D.) and the horizontal distances it traveled during the propulsive parts of each stroke (42.9±21.6 mm, mean ± S.D.), the intersection moved only slightly (2.5±2.8 mm, mean ± S.D.). As a consequence, the subsurface part of the leg appeared to pivot about the nearly

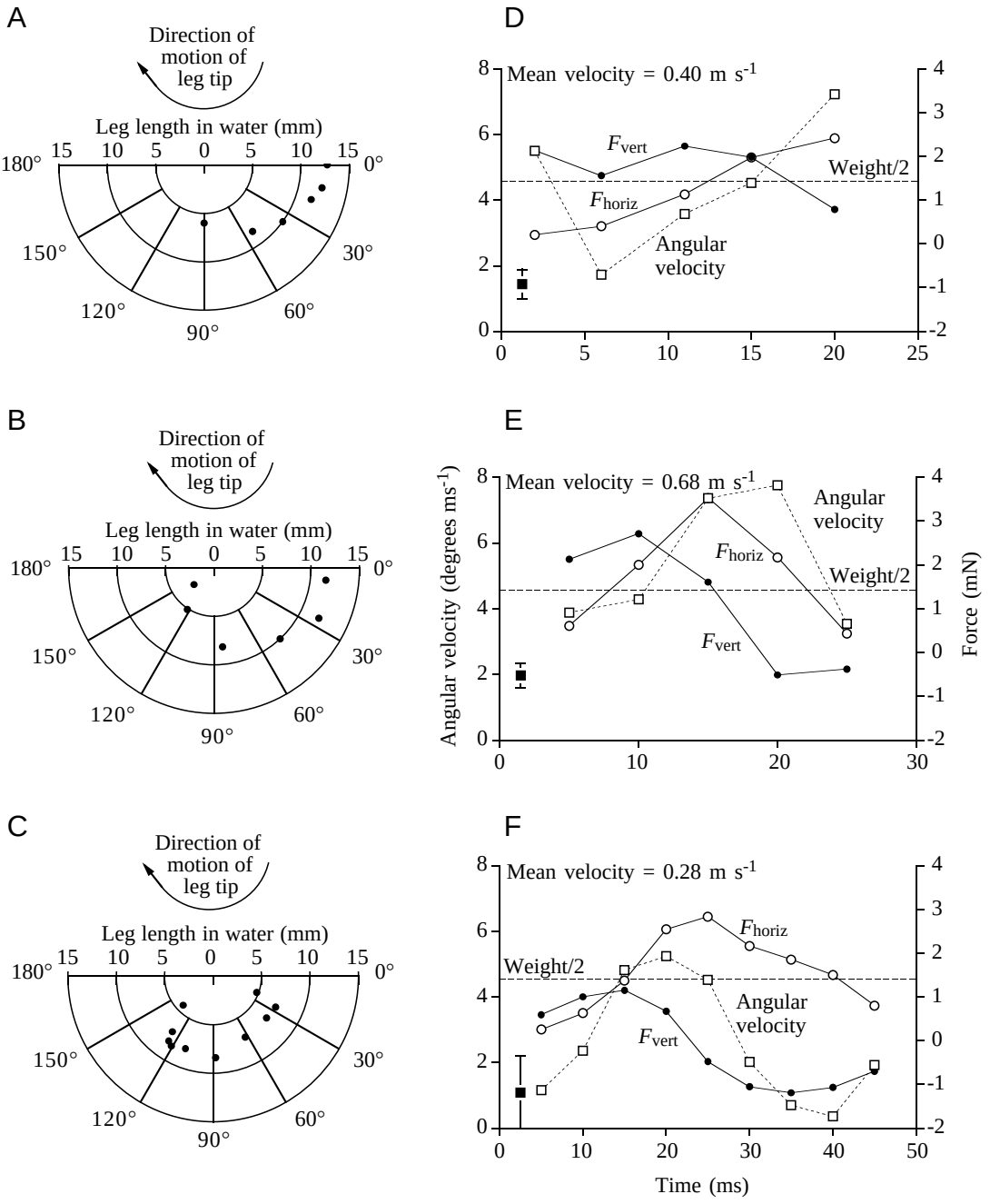


Fig. 15. A galloping spider sweeps the distal part of its propulsive legs below the water surface in a vertical plane, each leg tip tracing a complex arc (A–C) in which both its angle relative to the horizontal and its submerged length vary with time. During each sweep, the angular velocity of the leg tip in the vertical plane (□), varies substantially, whereas the angular velocity of the femur in the horizontal plane (■; mean ± S.D.) varies only slightly (D–F). We calculated both vertical (●) (equations 1 and 11) and horizontal (○) (equation 1) components of the thrust forces (D–F) generated during the sweeps by individual legs. A comparison of the vertical force on a leg on the surface, $F_{vert}$, for an individual leg with half the weight of the spider (horizontal dashed line; weight is halved because the propulsive legs act in pairs) shows that, during some strokes, $F_{vert}$ is insufficient to keep the spider airborne: the stroke depicted in F was followed immediately by the spider's descent to the water surface and the onset of rowing. $F_{horiz}$, horizontal component of thrust force.

stationary intersection between the leg and the water surface. This peculiar observation was the result of two motions: during a single propulsive stroke, the horizontal angular velocity of the femur (relative to the body) was 1.43±0.34 degrees $ms^{-1}$ (mean ± S.D., $N$=5; Fig. 15D–F), resulting in average horizontal velocities at the distal end of the femur of 0.17±0.04 $m\,s^{-1}$ (mean ± S.D.); during the same time period, flexion of the leg at the patella provided additional posteriad motion of the more distal leg segments (Fig. 15D–F).

*Horizontal and vertical thrust forces involved in galloping: calculations based on kinematic data*

As the propulsive (subsurface) part of the leg of a galloping spider pushed through the water, both its length and its angular velocity changed (Fig. 15), resulting in changes in the thrust (from drag) perpendicular to the direction of motion of the leg. The leg's angle relative to the water surface also changed during the stroke. We used equation 1 and the geometry of the leg's angle relative to the water surface to calculate and resolve the forces into their horizontal and vertical components (Figs 15D–F, 16). In these calculations, we assumed that the acceleration reaction was negligible, an assumption clearly not justified by the data (Fig. 15). Accordingly, our reported thrust forces are underestimates of the actual forces generated during galloping. The horizontal component of thrust (mean of values within a stroke) for a single propulsive leg varied from 0.87 to 1.77 mN (1.43±0.37 mN, mean ± S.D., $N$=6).

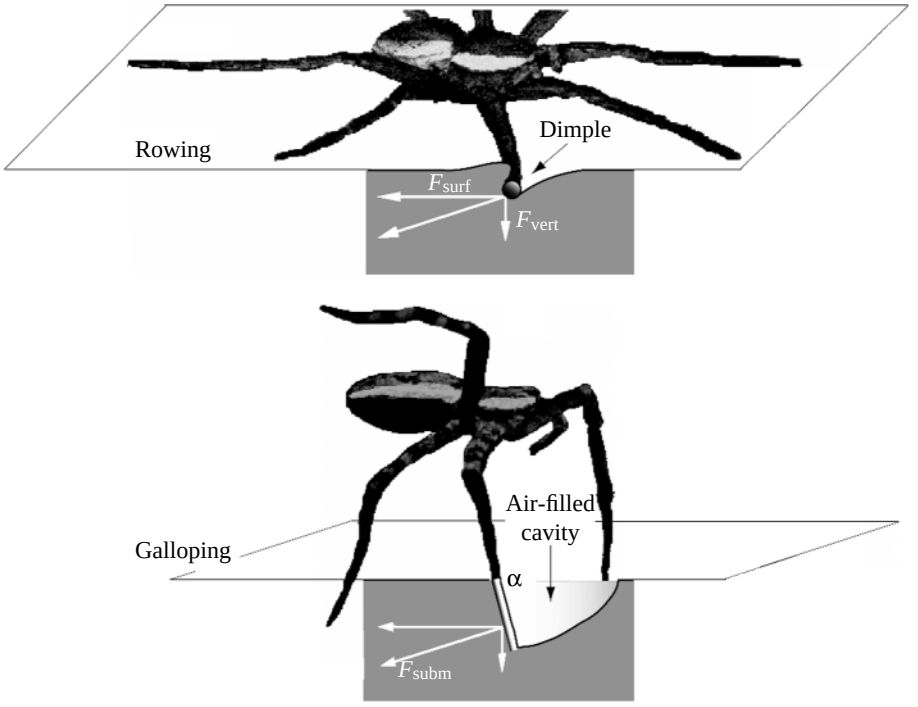


Fig. 16. Diagrammatic representations of the propulsive (horizontal; $F_{surf}$, $F_{subm}$) and supportive (vertical; $F_{vert}$) forces produced by *Dolomedes triton* during the propulsive phases of rowing and galloping. $F_{surf}$, the horizontal force produced by a leg at the surface; $F_{subm}$, the horizontal force produced by a submerged leg; $F_{vert}$, the vertical force on a leg on the surface; α, angle of a leg with respect to the water surface.

### *Comparison of rowing and galloping*

The rowing and galloping gaits of *D. triton* differed both in the motions used in locomotion and in the mechanisms of propulsion (Fig. 16): during rowing, the four propulsive legs were nearly horizontal and remained unflexed, whereas during galloping the six propulsive legs were flexed at the patella and only the femurs remained relatively horizontal; during rowing, the propulsive mechanism involved drag associated with the propulsive leg-cum-dimple being swept horizontally at a level just below the level of the undisturbed surface, whereas during galloping the propulsive mechanism involved drag associated with submerged propulsive legs moving in a vertical plane.

Rowing and galloping also differed quantitatively (Table 4): leg-tip velocity during galloping exceeded that during rowing by a factor of 3, the angular velocity of the femur during galloping exceeded that during rowing by approximately 70 %, and the horizontal thrust force generated (per leg pair) by a galloping spider exceeded that generated by a rowing spider by a factor of 3.8.

## Discussion

We have identified two classes of constraints on the rowing locomotion of *D. triton*: the efficacy of rowing is limited not only by the physical properties of the aquatic medium and of the air–water interface but also by the anatomy of the spider. The effect of these two sets of constraints is to force the spider to use a galloping gait, which is not similarly constrained, when it attempts to move at sustained velocities greater than $0.3\,m\,s^{-1}$.

### *Hydrodynamic and hydrostatic constraints on production of thrust during rowing*

Earlier experiments using segments of legs of *D. triton* on the surface of flowing water demonstrated that the horizontal forces generated by rowing spiders vary with dimple depth and with leg velocity (Suter et al., 1997). From the experiments reported here, we now know that the integrity of the dimple, a structure crucial in rowing, is limited: $d_{max}$ cannot exceed 3.8 mm under static conditions, and under dynamic conditions $d_{max}$ decreases linearly with increasing $U$ (Fig. 11, equation 10). This limit constrains spiders to a value of $F_{surf}$ that can be generated with a dimple depth that is less than the theoretical maximum. That thrust constraint is represented by a discontinuity in the surface defined by:

$$F_t = f(d,U) \quad (10)$$

(Fig. 14), where the location of the discontinuity is described

Table 4. *Comparison of rowing and galloping gaits for a 0.28 g* Dolomedes triton

| | Rowing | | Galloping | |
|---|---|---|---|---|
| | Value | Source | Value | Source |
| Horizontal propulsive force per pair of legs (mN) | 0.75 | Table 2 | 2.86 | *Kinematics of galloping* |
| Horizontal angular velocity of femur (degrees $ms^{-1}$) | 0.84 | Equation 3 | 1.43 | *Kinematics of galloping* |
| Leg-tip velocity ($m\,s^{-1}$) | 0.32 | Equation 3 | 0.98 | *Kinematics of galloping* |

by equation 10. In practice, this constraint means that a spider trying to row faster by pushing its legs deeper during every stroke must move its legs more slowly if the integrity of the dimples is to be preserved. Similarly, a spider trying to row faster by sweeping its legs faster must decrease the downward force of its legs, and therefore $d$, to preserve the dimples.

A second limitation to $d_{max}$ is related to the mass of the spider. As a spider pushes down with its propulsive legs and thereby produces a deeper dimple, it cannot make dimples so deep that the sum of their upward forces exceeds the weight of the spider: once the vertical force due to buoyancy and surface tension, $F_{vert}$, equals the weight of the spider, $M\boldsymbol{g}$, any further pushing downwards with the legs simply lifts the spider's body farther out of the water. In practice, this constraint is more restrictive for smaller spiders and poses no constraints on spiders exceeding 0.48 g (assuming that approximately one-third of each propulsive leg is used in propulsion). A spider trying to row faster by pushing its legs deeper during every stroke will find its efforts to push deeper frustrated by its insufficient weight.

The weight-limitation on $d_{max}$ constrains small spiders to parts of the surface, $F_t$ (Fig. 14B), that are nowhere intersected by the discontinuity described by equation 10. In contrast, much of the velocity/depth space that is physically and physiologically available to a spider exceeding 0.52 g is inferior because thrust is only available from a submerged leg segment, $F_{subm}$ (Fig. 14D).

The thrust forces ($F_{surf}$ and $F_{subm}$) generated during rowing by small *D. triton* are sufficient to provide intermittent propulsion at velocities that exceed those observed *in vivo*, but thrust forces generated by larger spiders are only just sufficient to propel them at velocities seen *in vivo*. Furthermore, no rowing spider can reach velocities as high as 0.3 m s$^{-1}$ averaged over several rowing strokes. In part, this limitation is a consequence of the submersion of the propulsive leg due to dimple disintegration, with the resulting decrease in force generated by each leg (Figs 12, 14). In part, however, the limitation results from the fact that, during the recovery phase of every rowing stroke, the spider's body and distal leg parts create drag as they support the spider on the water surface (Fig. 5; Table 1). Thus, the data show that the properties of water and of the air–water interface play important roles in limiting velocities attainable during rowing, thereby providing support for the drag-during-recovery hypothesis (hypothesis 2) and the dimple integrity hypothesis (hypothesis 3).

### *Anatomical constraints on the production of thrust during rowing*

Our comparison of the kinematics of rowing and galloping provides indirect evidence that the rowing gait of fishing spiders is also constrained by anatomy (hypothesis 1). During the propulsive phase of rowing, the horizontal angular velocity of the femur (Fig. 7B; Table 4) is approximately 60 % of the angular velocity of the femur during galloping, but leg-tip velocities during rowing are only 33 % of those during galloping. Because during rowing the spider keeps its legs nearly fully extended (Fig. 4A), it cannot add the angular velocity imparted by flexion at the proximal end of the femur to the angular velocity imparted by flexion at the femur's patellar end. We suspect that this is an anatomical constraint: the patellar joints move freely in the vertical plane but allow only limited flexion in other planes, and the resistance to twisting of the joints at the proximal end of the femur means that the dorsal surface of the propulsive leg can never face forwards. Thus, during rowing, flexions at both ends of the femur cannot be combined to produce high leg-tip velocities.

### *Gait-dependent constraints on velocity*

The rowing and galloping gaits differ in four ways: during rowing, (1) thrust is generated by four rather than six legs, (2) the water-engaged parts of the propulsive legs form dimples on the surface rather than being submerged during the power phase of the stroke, (3) the spider is always in contact with the water surface rather than being airborne for part of the time, and (4) even during the power phase of the stroke, non-propulsive parts of the spider are in contact with the water surface. Three of these (1, 3 and 4) constitute clear impediments to more rapid locomotion for a spider using the rowing gait: increasing the number of legs employed in generating thrust could raise $F_t$ by 50 %; being airborne during the glide phase of a stroke would eliminate water-based drag during that phase, thereby eliminating much of the deceleration encountered during rowing; and eliminating all non-propulsive contact with the water during the power phase of the stroke would also decrease water-based drag, thereby increasing net forward thrust.

The advantage of using a leg-cum-dimple (2) during rowing is indicated in part by the height of the discontinuity (Fig. 14) that separates the $F_{surf}$ and $F_{subm}$ surfaces. But the thrust difference between the two surfaces decreases as the leg moves more rapidly, and disappears at $U$>0.37 m s$^{-1}$, a velocity rarely attained by leg tips during rowing. So, if spiders were unconstrained by anatomy (above) and were therefore capable of moving their legs backwards as fast during rowing as they move during galloping, the thrust advantage associated with the maintenance of a dimple would be non-existent. Thus, it appears that anatomy constrains the fishing spider, during rowing, to leg-tip velocities at which the maintenance of a dimple is crucial for maximizing thrust (Fig. 14).

### *Gait change compelled by hydrodynamic constraints*

Our analysis indicates that the rowing gait of *D. triton* cannot, and does not (Fig. 3), propel the spider at velocities higher than 0.3 m s$^{-1}$. We have shown, in addition, that there are both anatomical and hydrodynamic constraints on the rowing gait. Galloping allows a spider to move considerably faster because, at the high leg-tip velocities that can be achieved when flexions at multiple leg joints are summed, the spider need not maintain the fragile structure of the dimple.

### List of symbols

| | |
|---|---|
| $A_f$ | frontal area (m) |
| $c$ | coefficient of power function |
| $C_d$ | drag coefficient |
| $d$ | depth of dimple (mm) |
| $d_{max}$ | maximum depth of dimple (mm) |
| f | function |
| $F$ | force (mN) |
| $F_{horiz}$ | horizontal component of thrust force (mN) |
| $F_{subm}$ | horizontal force, submerged leg (mN) |
| $F_{surf}$ | horizontal force, leg on the surface (mN) |
| $F_t$ | horizontal force, total (mN) |
| $F_{vert}$ | vertical force, leg on the surface (mN) |
| $\boldsymbol{g}$ | the acceleration due to gravity ($9.8\,m\,s^{-2}$) |
| $M$ | mass of spider (g) |
| $p$ | perimeter, leg–water contact (mm) |
| $Re$ | Reynolds number |
| $U$ | velocity of flow or leg ($m\,s^{-1}$) |
| $\alpha$ | angle of leg relative to water surface during galloping (degrees) |
| $\rho_f$ | density of the fluid ($kg\,m^{-3}$) |
| $\omega$ | angular velocity ($degrees\,ms^{-1}$) |

We thank Edgar Leighton at the University of Mississippi for providing us with the subjects of this study, Jessica Gruenwald for some of the data analysis, two anonymous reviewers for their remarkably thorough critiques and John Long both for his careful and very constructive comments on an earlier version of the manuscript and for the use of the high-speed videography equipment (provided to J. Long by grant N00014-97-1-0292 from the Office of Naval Research). The study was supported in part by funds provided by Vassar College through the Undergraduate Research Summer Institute and the Class of 1942 Faculty Research Fund.

### References

**Alexander, R. McN.** (1989). Optimization and gaits in the locomotion of vertebrates. *Physiol. Rev.* **69**, 1199–1227.

**Anderson, N. M.** (1976). A comparative study of locomotion on the water surface in semiaquatic bugs (Insects, Hemiptera, Gerromorpha). *Vidensk Meddr Dansk Naturh. Foren* **139**, 337–396.

**Barnes, W. J. P. and Barth, F. G.** (1991). Sensory control of locomotor mode in semi-aquatic spiders. In *Locomotor Neural Mechanisms in Arthropods and Vertebrates* (ed. D. M. Armstrong and B. M. H. Bush), pp. 105–116. Manchester: Manchester University Press.

**Batschelet, E.** (1981). *Circular Statistics in Biology*. London: Academic Press.

**Biewener, A. A. and Taylor, C. R.** (1986). Bone strain: A determinant of gait and speed? *J. Exp. Biol.* **123**, 383–400.

**Daniel, T. L.** (1984). Unsteady aspects of aquatic locomotion. *Am. Zool.* **24**, 121–134.

**Denny, M. W.** (1993). *Air and Water: The Biology and Physics of Life's Media*. Princeton: Princeton University Press.

**Deshefy, G. S.** (1981). 'Sailing' behaviour in the fishing spider, *Dolomedes triton* (Walckenaer). *Anim. Behav.* **29**, 965–966.

**Farley, C. T. and Taylor, C. R.** (1991). A mechanical trigger for the trot–gallop transition in horses. *Science* **253**, 306–308.

**Glasheen, J. W. and McMahon, T. A.** (1996a). A hydrodynamic model of locomotion in the Basilisk lizard. *Nature* **380**, 340–342.

**Glasheen, J. W. and McMahon, T. A.** (1996b). Size-dependence of water-running ability in basilisk lizards (*Basiliscus basiliscus*). *J. Exp. Biol.* **199**, 2611–2618.

**Gorb, S. N. and Barth, F. G.** (1994). Locomotor behavior during prey-capture of a fishing spider, *Dolomedes plantarius* (Araneae: Araneidae): Galloping and stopping. *J. Arachnol.* **22**, 89–93.

**Heglund, N. C. and Taylor, C. R.** (1974). Scaling stride frequency and gait to animal size: Mice to horses. *Science* **186**, 1112–1113.

**Heglund, N. C. and Taylor, C. R.** (1988). Speed, stride frequency and energy cost per stride: how do they change with body size and gait? *J. Exp. Biol.* **138**, 301–318.

**Hill, A. V.** (1950). The dimensions of animals and their muscular dynamics. *Sci. Prog.* **38**, 209–230.

**Hoyt, D. F. and Taylor, C. R.** (1981). Gait and the energetics of locomotion in horses. *Nature* **292**, 239–240.

**McAlister, W. H.** (1959). The diving and surface-walking behaviour of *Dolomedes triton sexpunctatus* (Araneida: Pisauridae). *Anim. Behav.* **8**, 109–111.

**McMahon, T. A.** (1985). The role of compliance in mammalian running gaits. *J. Exp. Biol.* **115**, 263–282.

**Shultz, J. W.** (1987). Walking and surface film locomotion in terrestrial and semi-aquatic spiders. *J. Exp. Biol.* **128**, 427–444.

**Suter, R. B.** (1999). Cheap transport for fishing spiders: the physics of sailing on the water surface. *J. Arachnol.* (in press).

**Suter, R. B., Rosenberg, O., Loeb, S., Wildman, H. and Long, J. H., Jr** (1997). Locomotion on the water surface: propulsive mechanisms of the fisher spider *Dolomedes triton*. *J. Exp. Biol.* **200**, 2523–2538.

**Taylor, C. R.** (1985). Force development during sustained locomotion: a determinant of gait, speed and metabolic power. *J. Exp. Biol.* **115**, 253–262.

**Vogel, S.** (1994). *Life in Moving Fluids* (second edition). Princeton: Princeton University Press.

**Webb, P. W.** (1973). Kinematics of pectoral fin propulsion in *Cymatogaster aggregata*. *J. Exp. Biol.* **59**, 697–710.

**Webb, P. W.** (1993). Swimming. In *The Physiology of Fishes* (ed. D. H. Evans), pp. 47–73. Boca Raton, FL: CRC Press.